

Exact Analysis of Rate Adaptation Algorithms in Wireless LANs

Angad Singh and David Starobinski

Department of Electrical and Computer Engineering, Boston University

Email: {*angad,staro*}@*bu.edu*

Abstract

Rate adaptation plays a key role in determining the performance of wireless LANs. In this paper, we introduce a semi-Markovian framework to analyze the performance of two of the most popular rate adaptation algorithms used in wireless LANs, namely Automatic Rate Fallback (ARF) and Adaptive Automatic Rate Fallback (AARF). Given our modeling assumptions, the analysis is exact and provides closed form expressions for the achievable throughput of ARF and AARF. We illustrate the benefit of our analysis by numerically comparing the throughput performance of ARF and AARF in two different channel regimes. The results show that neither of these algorithms consistently outperforms the other. We thus propose and analyze a new variant to AARF, called Persistent AARF (or PAARF), and show that it achieves a good compromise between the two algorithms, often performing close to the best algorithm in each of the studied regimes. The numerical results also shed light into the impact of MAC overhead on the performance of the three algorithms. In particular, they show that the more conservative strategies AARF and PAARF scale better as the bit rate increases.

I. INTRODUCTION

Wireless LANs play a prominent role among wireless communication systems [1], [2], [3]. Most wireless LANs support data transmission at multiple bit rates by employing different modulation and channel encoding schemes. The IEEE 802.11 WLAN family of standards is amongst the most popular WLAN systems supporting data transmission at multiple bit rates [2], [4]. For instance, the IEEE 802.11b standard allows transmissions at four different bit rates, i.e., 1, 2, 5.5, and 11 Mbs, while the newer IEEE 802.11g standard allows transmissions at 12 different bit rates ranging from 1 Mbs to 54 Mbs.

The volatile nature of the wireless channel resulting from fading, attenuation, and interference from other radiation sources, makes the task of rate selection in multi-rate WLANs system a key feature for throughput optimization. A well designed algorithm ought to select a bit rate for data transmission that maximizes the instantaneous throughput. A key challenge however is that channel quality usually fluctuates and, thus, any rate selection algorithm must adapt to variations in the channel and network conditions.

For IEEE 802.11 WLAN systems, several rate adaptation algorithms have been proposed, see, e.g., [5], [6], [7], [8], [9], [10]. Most of these algorithms are rooted in the same design philosophy. They employ open-loop rate adaptation schemes, run locally on the network nodes, that dynamically determine the data transmission rate based on certain statistics collected by the transmitting node. Two of the most popular rate adaptation algorithms belonging to this category are the Automatic Rate Fallback (ARF) [5] and Adaptive Automatic Rate Fallback (AARF) [6] algorithms that use consecutive successful or failed packet transmissions to guide rate adaptation (cf. Section II).

In this paper, we propose a new analytical framework to evaluate the performance of the ARF and AARF algorithms in wireless LANs with random channels. Our analysis, based on the theory of semi-Markov processes [11], is *exact* and provides *closed-form* expressions for the throughput achieved by ARF and AARF. While our analysis necessarily relies on some simplifying assumptions for the sake of tractability, it has the clear advantage of providing meaningful insight into the impact of various algorithm and channel parameters on the performance of these algorithms.

To illustrate the benefits of our analysis, we present numerical results comparing the performance ARF and AARF for different channel regimes. Our numerical results clearly identify channel regimes where AARF outperforms ARF, and are in line with simulation and experimental results reported in [10],

[6]. More surprisingly, they also show that there exist some practical regimes where ARF significantly outperforms AARF.

Based on the insights gathered from our numerical analysis, we propose a new variant to AARF, called Persistent Adaptive Automatic Rate Fallback (PAARF). We show that the analysis of AARF can easily be extended to that of PAARF. Numerical results show that PAARF reaches a good compromise between ARF and AARF and often gets very close to the best performing algorithm in each of the studied regimes.

It should be emphasized that the main goal of this paper is to provide general, qualitative insight into the performance of rate adaption algorithms in wireless LANs, rather than conducting detailed numerical modeling of a specific protocol.

The rest of this paper is organized as follows. We discuss related work in Section II and introduce our model and notations in Section III. We conduct the analysis of ARF and AARF in Section IV and show how it can be generalized to handle MAC overhead. In Section V, we numerically compare the performance of ARF and AARF and introduce the new PAARF algorithm. We provide concluding remarks in Section VI.

II. RELATED WORK

We first provide detail on the ARF and AARF algorithm and then briefly discuss other relevant work. ARF [5] is the first documented rate adaptation algorithm developed to optimize throughput performance in wireless LAN devices. ARF keeps transmitting at a given bit rate until a certain number of *consecutive* packets transmissions have either succeeded or failed. Specifically, if f consecutive packet transmissions fail to get acknowledged at the current bit rate, then the next lower bit rate (if there is such one) is selected for data transmission. Similarly, if s consecutive packet transmissions are acknowledged without any re-transmissions at the current bit rate, then the next higher bit rate (if there is such one) is selected for data transmission. The default value of ARF parameters are $f = 2$ and $s = 10$. ARF requires the maintenance of very little state information. Its simplicity has made it one of the most widely implemented open-loop rate adaptation schemes in commercial 802.11 WLAN devices [9].

AARF [6] is derived from ARF. It tries to improve throughput performance in scenarios where the packet success probability at a certain bit rate is much higher than at the next higher bit rate. The problem with ARF in such cases is that after s consecutive successful packet transmission at the low bit rate it

always attempts transmissions at the higher bit rate. Instead, AARF implements a binary exponential back-off procedure whereby after every failed probe packet transmission at the higher bit rate, AARF doubles (up to some maximum value) the threshold number of consecutive packet transmissions required at the current bit rate before attempting a packet transmission at the next higher bit rate. Thus, AARF initially looks for s consecutive successful packet transmissions at the current bit rate after which it sends a probe packet at the next higher bit rate. If the probe packet transmission is successful, then AARF switches to the higher bit rate. Otherwise, it stays in the current bit rate. In that case, the next probe packet transmission at the higher bit rate is attempted only after $2s$ consecutive successful packet transmissions at the current bit rate and so forth.

Several papers have proposed various modifications and improvements over the basic ARF and AARF rate adaptation algorithms, see e.g., [10], [8], [9], [12], [13]. Several of these algorithms, e.g., [9], [12], [13], are based on variations of ARF, and thus we expect our analytical models to be useful to evaluate their performance as well.

So far, most of the evaluation of rate adaptation algorithms has been carried out through simulations [6], [9], [7], [14], [15], [13], [16] or experiments on actual testbed networks [10], [8]. Although there exists analytical work for multi-rate wireless networks, see e.g., [17], [18], that work assumes that each node always transmits at a fixed rate. An exception is the recent work of [19], where, among other contributions, the authors present a Markov chain model of ARF. The present work differs from [19] in several aspects. First, we use the more general theory of semi-Markov processes to analyze rate adaptation algorithms. Thus, the analysis provides means to evaluate the effects of MAC overhead (e.g., binary exponential back-off), which can be significant at high bit rate rates. Second, we also provide an analysis of the AARF algorithm and numerical comparisons between the performance of ARF and AARF. Finally, we introduce the new PAARF algorithm and compare its performance to the two other algorithms. A preliminary version of this paper appeared in [20]. The present work primarily adds to that earlier work by modeling and analyzing the impact of MAC overhead (cf. Sections IV-C and V-C).

III. MODEL AND NOTATIONS

Our goal in this paper is to conduct an exact analysis of the performance of the ARF and AARF algorithms in wireless LANs, such as IEEE 802.11 networks. As such, a certain number of assumptions are necessary in order to keep the analysis tractable.

In order to decouple the behavior of the above algorithms from other MAC and higher-layer mechanisms, we focus our attention on the behavior of ARF and AARF for a single source-destination pair (e.g., a mobile node and a base station). We note that most wireless LANs operate at low load and, thus, it is typical that, at any given point of time, only one pair of nodes communicates [21]. We assume that the source is greedy, i.e., it has always packets to transmit.

The source can transmit packets at N different bit rates, denoted by R_1, R_2, \dots, R_N in units of bit/s. Without any limitations of generality, we assume that these rates are sorted from the lowest to the highest, i.e., R_1 represents the lowest available bit rate and R_N the highest. At each bit rate R_i , we denote the probability of a successful packet transmission by α_i , where $0 < \alpha_i < 1$. This probability is assumed to be independent of any other events.

We use the random variable ℓ to represent the length (in bits) of a packet. This variable follows an arbitrary i.i.d. distribution (i.e., not necessarily exponential). The mean packet length is denoted by $\bar{\ell}$.

Next, define f_i to be the long run proportion of time during which packet transmission is carried out at the bit rate R_i . We can then express the steady-state throughput τ as follows:

$$\tau = \sum_{i=1}^N f_i \alpha_i R_i. \quad (1)$$

The key for characterizing the throughput performance of ARF and AARF resides in deriving an expression for f_i for each of the algorithms.

IV. ANALYSIS

In Sections IV-A and IV-B, we analyze the throughput performance of ARF and AARF. The analysis will lead to closed-form expressions for the throughput delivered by these algorithms. The focus of the analysis presented in these sections is to understand the basic behavior of these algorithms independent of the specific underlying MAC protocol. Hence, initially, we will not deal with protocol-specific details, such as back-off retransmissions, control packets, and inter-frame spacings in the analysis. Those will be considered in Section IV-C.

A. ARF

Based on our statistical assumptions, we next show that the behavior of ARF can be analyzed using the theory of semi-Markov processes [11]. Similar to a Markov process, a semi-Markov process transitions

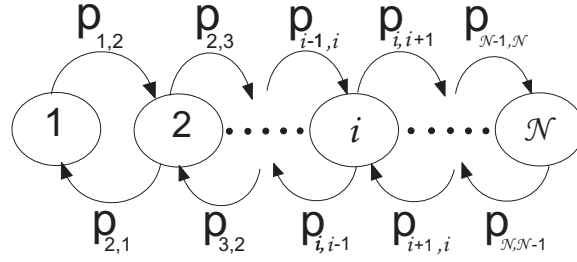


Fig. 1. Embedded Markov chain modeling ARF behavior at the moments of transitions to a new state. State i represents packet transmissions at rate R_i .

between different states. Upon *entering* a certain state, the time spent in that state and the transition probabilities to the various possible next states depend only on the present state and are independent of the history. However, contrary to a standard Markov process, the time spent in each state follows a general distribution, which is not necessarily memoryless. Thus, a semi-Markov process is not Markovian at an arbitrary point of time. However, one can create an embedded Markov chain by sampling the original process at moments of transition to a new state.

Now, define state i to be the state in which packets are transmitted at the bit rate R_i . Clearly, upon entering state $2 \leq i \leq N - 1$, the time spent in that state and the transition probabilities to state $i - 1$ and $i + 1$ depend only on the parameters α_i , R_i , $\bar{\ell}$, s , and f and, thus, are independent of the past. Similar arguments apply for the time spent in states 1 and N . Thus, the behavior of ARF can be modeled using a semi-Markov process. The embedded Markov chain for the problem at hand is depicted in Fig. 1. The quantities $p_{i,j}$ shown in the figure represent the transition probabilities from state i to state j .

As per Eq. (1), in order to find an expression for the throughput of ARF we need to calculate f_i , i.e., the long run proportion of time data transmission is carried out at the bit rate R_i . Let p_i represent the steady-state probability of finding the semi-Markov process in state i . From the definition of state i , we immediately see that $f_i = p_i$.

In order to compute p_i , we will exploit the mathematical properties of semi-Markov processes [11]. Specifically, define μ_i to be the mean time spent in each state i of the semi-Markov process and π_i to be the steady-state proportion of transitions into state i . The latter also corresponds to the steady-state fraction of time the embedded Markov chain associated with the process finds itself in state i . Then, it can be shown [11]:

$$p_i = \frac{\pi_i \mu_i}{\sum_{i=1}^N \pi_i \mu_i}. \quad (2)$$

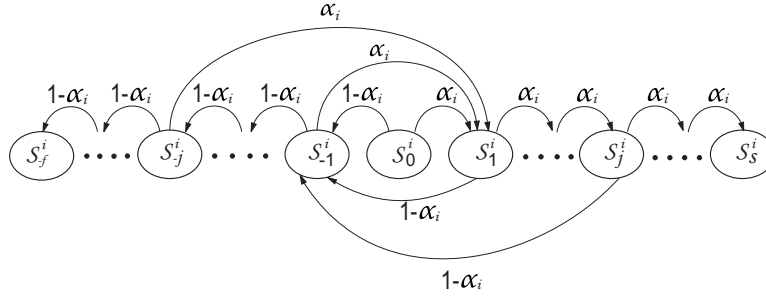


Fig. 2. ARF operation at an intermediate bit rate R_i . States S_j^i and S_{-j}^i represent respectively j consecutive successful and failed packet transmissions.

The embedded Markov chain shown in Fig. 1 is a simple birth-death process [11]. Thus, the steady-state probabilities π_i , for each state $i \geq 2$, can readily be expressed as follows:

$$\pi_i = \pi_1 \prod_{k=1}^{i-1} \frac{p_{k,k+1}}{p_{k+1,k}}. \quad (3)$$

In order to calculate π_1 , we apply the normalization condition and get

$$\pi_1 = \frac{1}{1 + \sum_{i=2}^N \prod_{k=1}^{i-1} \frac{p_{k,k+1}}{p_{k+1,k}}}. \quad (4)$$

In order to complete the analysis, it just remains to derive expression for the average time spent in each state μ_i and the transition probabilities $p_{i,j}$. Toward this end, we need to model the operations of ARF within each state i , corresponding to transmissions at bit rate R_i . Specifically, we need to keep track of the number of consecutive successful or failed packet transmissions. The state diagram shown in Fig. 2 models the behavior of ARF at a given bit rate R_i , where $1 < i < N$. The initial state is state S_0^i . Each subsequent successful packet transmission leads to a transition into some state S_j^i , where j represents the number of consecutive successful packet transmissions. Similarly each failed packet transmission leads to a transition into some state S_{-j}^i where j represents the number of consecutive failed packet transmissions. States S_s^i and S_{-f}^i are termination states after which packet transmissions will occur at bit rates R_{i+1} and R_{i-1} , respectively. The state diagrams for bit rates R_1 and R_N are similar, except that there is no need to account for consecutive failed packet transmissions and consecutive successful packet transmissions, respectively.

Now, let the random variable $X_i(j)$ represent the number of packet transmissions at bit rate R_i before reaching state S_s^i or state S_{-f}^i , starting from state S_j^i . The quantity $\overline{X}_i(0)$ represents the average number of packet transmission starting from state S_0^i until one of the termination states is reached. One can

express μ_i as a function of $\overline{X}_i(0)$ in the following way:

$$\mu_i = \overline{X}_i(0) \frac{\bar{\ell}}{R_i}. \quad (5)$$

The special structure of the state diagram shown in Fig. 2 allows to provide a closed-form expression for $\overline{X}_i(0)$, as given by the following proposition.

Proposition 1 *Let $\overline{X}_i(0)$ represents the expected number of packet transmission in state i of Fig. 1. Then, the following holds:*

$$\overline{X}_i(0) = \begin{cases} \frac{\sum_{j=0}^{s-1} (\alpha_i)^j}{(\alpha_i)^s}, & \text{for } i = 1; \\ \frac{\sum_{j=0}^{s-1} (\alpha_i)^j \sum_{j=0}^{f-1} (1-\alpha_i)^j}{1 - \sum_{j=1}^{s-1} (\alpha_i)^j \sum_{j=1}^{f-1} (1-\alpha_i)^j}, & \text{for } 1 < i < N \text{ with } s > 1 \text{ and } f > 1; \\ \sum_{j=0}^{s-1} (\alpha_i)^j \sum_{j=0}^{f-1} (1-\alpha_i)^j, & \text{for } 1 < i < N \text{ with } s = 1 \text{ or } f = 1; \\ \frac{\sum_{j=0}^{f-1} (1-\alpha_i)^j}{(1-\alpha_i)^f}, & \text{for } i = N. \end{cases} \quad (6)$$

Proof:

We will prove the proposition for the case $1 < i < N$ with $s > 1$ and $f > 1$. The proof for the other cases is similar.

The proof follows a two step approach. The first step is to show that the following two equations hold:

$$\overline{X}_i(s-u) = \sum_{k=1}^u (\alpha_i)^k + (1-\alpha_i)(1 + \overline{X}_i(-1)) \sum_{k=0}^{u-1} (\alpha_i)^k, \quad \text{for } 0 < u < s; \quad (7)$$

$$\overline{X}_i(-f+v) = \sum_{k=1}^v (1-\alpha_i)^k + \alpha_i(1 + \overline{X}_i(1)) \sum_{k=0}^{v-1} (1-\alpha_i)^k, \quad \text{for } 0 < v < f. \quad (8)$$

We will prove Eq. (7) using mathematical induction. The proof of Eq. (8) is conducted in a similar manner.

First, we prove the basis of the induction, i.e., we consider the case $u = 1$. Consider the average number of transmissions starting from state \mathcal{S}_{s-1}^i . With probability α_i , the next packet transmission is successful and ARF exits the current bit rate to the next higher bit rate. Otherwise, with probability $1 - \alpha_i$, the transmission fails and the process moves to state \mathcal{S}_{-1}^i . We thus have

$$\overline{X}_i(s-1) = \alpha_i \cdot 1 + (1-\alpha_i)(1 + \overline{X}_i(-1)). \quad (9)$$

This equation is equivalent to Eq. (7) for $u = 1$ and thus proves the basis of the induction.

Next, we prove the induction step. Assume Eq. (7) holds true for $u = m$, where $1 \leq m < s - 1$, that

is,

$$\overline{X}_i(s-m) = \sum_{k=1}^m (\alpha_i)^k + (1-\alpha_i)(1 + \overline{X}_i(-1)) \sum_{k=0}^{m-1} (\alpha_i)^k. \quad (10)$$

Now assume that the process is in state $\mathcal{S}_{s-(m+1)}^i$. With probability α_i , the next transmission is successful and the process moves to state \mathcal{S}_{s-m}^i . Otherwise, with probability $1-\alpha_i$, the transmission fails and the process moves to state \mathcal{S}_{-1}^i . Thus,

$$\overline{X}_i(s-(m+1)) = \alpha_i(1 + \overline{X}_i(s-m)) + (1-\alpha_i)(1 + \overline{X}_i(-1)). \quad (11)$$

Substituting Eq. (10) into Eq. (11), we obtain

$$\overline{X}_i(s-(m+1)) = \sum_{k=1}^{m+1} (\alpha_i)^k + (1-\alpha_i)(1 + \overline{X}_i(-1)) \sum_{k=0}^m (\alpha_i)^k, \quad (12)$$

hence proving the induction step.

Now we proceed with the second step of the proof. We note that after the process enters state \mathcal{S}_0^i , it either moves to state \mathcal{S}_1^i (with probability α_i) or to state \mathcal{S}_{-1}^i (with probability $1-\alpha_i$). Therefore,

$$\overline{X}_i(0) = \alpha_i(\overline{X}_i(1) + 1) + (1-\alpha_i)(\overline{X}_i(-1) + 1). \quad (13)$$

Substituting $u = s-1$ in Eq. (7) and $v = f-1$ in Eq. (8), we get

$$\overline{X}_i(1) = \sum_{k=1}^{s-1} (\alpha_i)^k + (1-\alpha_i)(1 + \overline{X}_i(-1)) \sum_{k=0}^{s-2} (\alpha_i)^k; \quad (14)$$

$$\overline{X}_i(-1) = \sum_{k=1}^{f-1} (1-\alpha_i)^k + \alpha_i(1 + \overline{X}_i(1)) \sum_{k=0}^{f-2} (1-\alpha_i)^k. \quad (15)$$

Equations (13), (14) and (15) provide three linear equations in three unknowns (i.e., $\overline{X}_i(0)$, $\overline{X}_i(-1)$ and $\overline{X}_i(1)$) from which obtain the expression of $\overline{X}_i(0)$ given by Proposition 1 for the case $1 < i < N$ with $s > 1$ and $f > 1$. ■

The next proposition provides expressions for the transition probabilities of the embedded Markov chain shown in Fig. 1, for $1 < i < N$. To prove this proposition, we compute the probability of getting from state \mathcal{S}_0^i to state \mathcal{S}_s^i , which corresponds exactly to $p_{i,i+1}$.

Proposition 2 *Let $p_{i,i+1}$ be the transition probability of switching from state i to state $i+1$. Then,*

$$p_{i,i+1} = \begin{cases} \frac{(\alpha_i)^s \sum_{j=0}^{f-1} (1-\alpha_i)^j}{1 - [\sum_{j=1}^{s-1} (\alpha_i)^j \sum_{j=1}^{f-1} (1-\alpha_i)^j]} & \text{for } 1 < i < N \text{ with } s > 1 \text{ and } f > 1; \\ (\alpha_i)^s \sum_{j=0}^{f-1} (1-\alpha_i)^j & \text{for } 1 < i < N \text{ with } s = 1 \text{ or } f = 1. \end{cases} \quad (16)$$

In addition, we have $p_{1,2} = p_{N,N-1} = 1$, and $p_{i,i-1} = 1 - p_{i,i+1}$ for $1 < i < N$.

Proof:

Define $q_i(j)$ to be the probability of reaching state \mathcal{S}_s^i from state \mathcal{S}_j^i . Therefore, $p_{i,i+1} = q_i(0)$.

We outline the proof of the proposition for the case $1 < i < N$ with $s > 1$ and $f > 1$. Similar to Proposition 1, the proof follows a two step approach. The first step is to prove that the following two equations hold, which can be done via induction as in the proof of Proposition 1:

$$q_i(s-u) = \alpha_i^u + q_i(-1)(1-\alpha_i) \sum_{k=0}^{u-1} \alpha_i^k \text{ for } 0 < u < s; \quad (17)$$

$$q_i(-(f-v)) = q_i(1)\alpha_i \sum_{k=0}^{v-1} (1-\alpha_i)^k \text{ for } 0 < v < f. \quad (18)$$

Next, we note that

$$q_i(0) = \alpha_i q_i(1) + (1-\alpha_i)q_i(-1), \quad (19)$$

and substituting $u = s-1$ in Eq. (17) and $v = f-1$ in Eq. (18) we have,

$$q_i(1) = \alpha_i^{s-1} + q_i(-1)(1-\alpha_i) \sum_{k=0}^{s-2} (\alpha_i)^k; \quad (20)$$

$$q_i(-1) = q_i(1)\alpha_i \sum_{k=0}^{f-2} (1-\alpha_i)^k. \quad (21)$$

Solving Eqs. (19), (20) and (21) for $q_i(0)$, we obtain the expression of $p_{i,i+1}$ given by Proposition 2 for the case $1 < i < N$ with $s > 1$ and $f > 1$. ■

Using Eqs. (2), (3), (4), (5) and Propositions 1 and 2, we thus have derived closed-form expressions for p_i , where $1 \leq i \leq N$, as a function of the parameters $\alpha_i, R_i, \bar{\ell}, s, f$ and N . Since $f_i = p_i$, an expression for the throughput of ARF follows immediately from Eq. (1).

B. AARF

The behavior of AARF is conceptually similar to that of ARF and its analysis can also be carried out using a semi-Markov process formulation. The complexity of the analysis lies in modeling the back-off procedure of AARF, which requires properly defining the states of the semi-Markov process.

To model the operation of AARF at each bit rate R_i , where $1 \leq i \leq N$, we define the ‘‘fall back’’ states i_β and the ‘‘probe states’’ i_β^{+1} , as illustrated in Fig. 3. The variable β , where $0 \leq \beta \leq \beta_{max}$, is

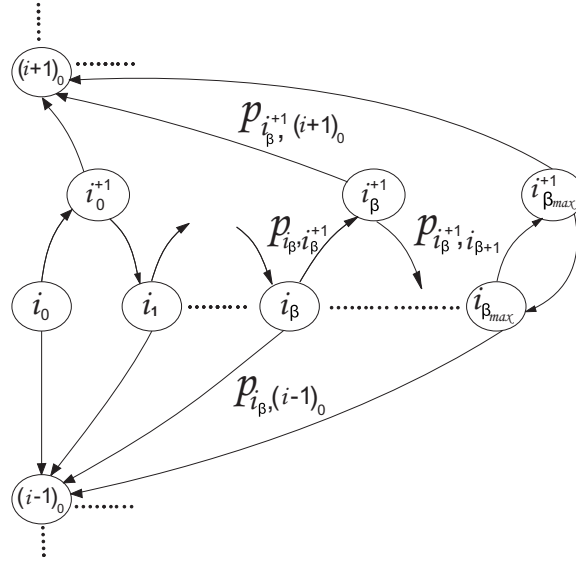


Fig. 3. Embedded Markov chain modeling AARF behavior at the moments of transitions to a new state. The variable β is an indicator of the back-off stage. States i_{β} correspond to “fall back” states, in which transmissions take place at rate R_i , and states i_{β}^{+1} correspond to “probe states”, in which transmissions take place at rate R_{i+1} .

indicative of the current back-off stage. Thus, if the process is in state i_{β} , there must be $2^{\beta}s$ consecutive successful packet transmissions before the process moves to probe state i_{β}^{+1} , where a probe packet is transmitted at rate R_{i+1} . If the probe packet is successfully transmitted then the process transitions to state $(i+1)_0$. Otherwise, the process moves to the next fall back state, i.e., state $i_{\beta+1}$. Similar to ARF, if the process is in some state i_{β} and experiences f consecutive packet transmission failures then it transitions to state $(i-1)_0$ (except for the case $i=1$, where the process remains in the same state). The state $i_{\beta_{max}}$ represents the maximum fall back state. The process keeps returning to that state until the transmission of a probe packet at rate R_{i+1} is successful or f consequent packet failures occur. Finally, we note that there are no fall back states at rate R_N , and thus there is only one state N_0 which is defined the same way as state N in ARF.

Similar to ARF, whenever the process enters one of the above defined states, the time spent in each state and the transition probabilities to the next possible states are independent of the history. Thus, the behavior of AARF can be modeled using a semi-Markov process. The embedded Markov chain for this process is shown in Fig. 3.

As per Eq. (1), in order to find an expression for the throughput of AARF, we need to calculate f_i , i.e., the long run proportion of time data transmission is carried out at the bit rate R_i . The quantities

f_i can be expressed as a function of p_{i_β} and $p_{(i-1)_\beta}^{+1}$ which are defined as the steady-state probabilities of finding the semi-Markov process in either the fall-back state i_β or the probe packet state $(i-1)_\beta^{+1}$ respectively. Specifically, we have

$$f_i = \sum_{\beta=0}^{\beta_{max}} (p_{i_\beta} + p_{(i-1)_\beta}^{+1}) \quad \text{for } 1 \leq i \leq N, \quad (22)$$

where by definition $p_{0_\beta}^{+1} = 0$, and $p_{N_\beta} = 0$ for $\beta \geq 1$.

As in the previous section, we can find expressions for p_{i_β} and $p_{i_\beta}^{+1}$ by computing i) the average time spent in each state of the semi-Markov process; ii) the transition probabilities of the embedded Markov chain; and iii) the steady-state probabilities of the embedded Markov chain.

We start with items i) and ii). Consider first the probe states. The average time spent in state i_β^{+1} is simply $\mu_{i_\beta}^{+1} = \bar{\ell}/R_{i+1}$. The transition probabilities out of the probe states, for $\beta < \beta_{max}$, are given by $p_{(i_\beta^{+1}, (i+1)_0)} = \alpha_{i+1}$ and $p_{(i_\beta^{+1}, i_{\beta+1})} = 1 - \alpha_{i+1}$. For the case $\beta = \beta_{max}$, we have $p_{(i_{\beta_{max}}^{+1}, (i+1)_0)} = \alpha_{i+1}$ and $p_{(i_{\beta_{max}}^{+1}, i_{\beta_{max}})} = 1 - \alpha_{i+1}$.

The behavior of AARF in the fall back states i_β is very similar to that of ARF in state i , except that the number of consecutive successful transmissions required before transmitting at the next higher bit rate is $b_\beta = 2^\beta s$ instead of just s . Thus, we can obtain an expression for μ_{i_β} by simply replacing s by b_β in Proposition 1.

The last item to complete the analysis is to compute the steady-state probabilities of the embedded Markov chain π_{i_β} and $\pi_{i_\beta}^{+1}$. Once this is done, the proportion of time spent by AARF in each state is given by the following expressions that are analogous to Eq. (2):

$$p_{i_\beta} = \frac{\pi_{i_\beta} \mu_{i_\beta}}{\sum_{i=1}^N \sum_{\beta=1}^{\beta_{max}} (\pi_{i_\beta} + \pi_{(i-1)_\beta}^{+1})}; \quad p_{i_\beta}^{+1} = \frac{\pi_{i_\beta}^{+1} \mu_{i_\beta}^{+1}}{\sum_{i=1}^N \sum_{\beta=1}^{\beta_{max}} (\pi_{i_\beta} + \pi_{(i-1)_\beta}^{+1})}, \quad (23)$$

where by definition $\pi_{0_\beta}^{+1} = 0$, and $\pi_{N_\beta} = 0$ for $\beta \geq 1$.

We next show that the seemingly complex structure of the embedded Markov chain shown in Fig. 3 has the remarkable property of collapsing into a simple birth-death process.

First, we observe that the steady probabilities of the states at level i , namely π_{i_β} and $\pi_{i_\beta}^{+1}$, can all be expressed as a function of π_{i_0} . This is done by taking contours around each state of level i in order, that is, $i_0^{+1}, i_1, i_1^{+1}, \dots$, and writing the balance equations for each. The expressions are as follows:

$$\pi_{i_\beta}^{+1} = \begin{cases} \pi_{i_0} p_{(i_\beta, i_\beta^{+1})} \prod_{k=0}^{\beta-1} [p_{(i_k, i_k^{+1})} p_{(i_k^{+1}, i_{k+1})}], & \text{for } 0 \leq \beta < \beta_{max} \text{ and } 1 \leq i < N; \\ \frac{\pi_{i_0} p_{(i_\beta, i_\beta^{+1})} \prod_{k=0}^{\beta-1} [p_{(i_k, i_k^{+1})} p_{(i_k^{+1}, i_{k+1})}]}{1 - p_{(i_\beta^{+1}, i_\beta)} p_{(i_\beta, i_\beta^{+1})}}, & \text{for } \beta = \beta_{max} \text{ and } 1 \leq i < N; \end{cases} \quad (24)$$

$$\pi_{i_\beta} = \begin{cases} \pi_{i_0} \prod_{k=0}^{\beta-1} [p_{(i_k, i_k^{+1})} p_{(i_k^{+1}, i_{k+1})}], & \text{for } 0 < \beta < \beta_{max} \text{ and } 1 \leq i < N; \\ \frac{\pi_{i_0} \prod_{k=0}^{\beta-1} [p_{(i_k, i_k^{+1})} p_{(i_k^{+1}, i_{k+1})}]}{1 - p_{(i_\beta^{+1}, i_\beta)} p_{(i_\beta, i_\beta^{+1})}}, & \text{for } \beta = \beta_{max} \text{ and } 1 \leq i < N. \end{cases} \quad (25)$$

Now, at equilibrium, the rate of transitions from level i to level $i + 1$ must be the same as that from level $i + 1$ to level i . Thus,

$$\sum_{\beta=0}^{\beta_{max}} (p_{i_\beta^{+1}, (i+1)_0}) \pi_{i_\beta}^{+1} = \sum_{\beta=0}^{\beta_{max}} (p_{(i+1)_\beta, i_0}) \pi_{(i+1)_\beta}, \quad \text{for } 1 \leq i < N. \quad (26)$$

Using Eq. (24), all the individual terms in the lhs of Eq. (26) can be expressed as a function of π_{i_0} , while, using Eq. (25), all the individual terms in the rhs of Eq. (26) can be expressed as a function of $\pi_{(i+1)_0}$, leading to balance equations similar to a birth-death process. Using Eq. (26), we can then express all the steady-state probabilities as a function of π_{i_0} . Finally, we can resort to the normalization condition to evaluate π_{i_0} , i.e.,

$$\sum_{i=1}^N \sum_{\beta=0}^{\beta_{max}} (\pi_{i_\beta} + \pi_{(i-1)_\beta}^{+1}) = 1, \quad (27)$$

and our analysis is complete.

C. Accounting for MAC Overhead

We now outline a generalization of the previous analysis to account for the MAC overhead present in real protocols. We focus on the popular IEEE 802.11b DCF standard [2], with which we assume the reader is familiar. For brevity, we only discuss the ARF algorithm, since the generalized analysis of AARF follows similar lines. Due to space constraints, detailed technical derivations are deferred to [22].

The first source of overhead in IEEE 802.11 is the transmission time of ACK packets, denoted by T_{ACK} , and the required inter-frame spacings DIFS and SIFS. For simplicity, we assume that the RTS/CTS handshake is disabled and ACK packets are not lost. Hence, for each successful DATA packet transmission, the time overhead amounts to $T_{success} = DIFS + SIFS + T_{ACK}$, while for each failed DATA packet transmission, the overhead corresponds to $T_{failure} = DIFS$.

The second major source of overhead results from the binary exponential back-off procedure. The average back-off time, after $0 \leq \gamma \leq \gamma_{max}$ consecutive failures, is given by:

$$\bar{T}_b(\gamma) = \frac{2^\gamma CW_{min} - 1}{2}, \quad (28)$$

where γ is the back-off counter. The value of this counter is incremented after each transmission failure and reset after a successful transmission. Note that γ_{max} represents the maximum number of retransmission attempts before the packet is dropped. We assume that $CW_{max} \geq 2^{\gamma_{max}} CW_{min} - 1$.

We now model the evolution of the ARF process, inclusive of MAC overhead. We define i_γ to be a state of the process in which packet transmissions are carried out at the bit rate R_i . The index γ corresponds to the value of the back-off counter *at the instant* where the process enters the state. Transitions out of state i_γ take place when the bit rate changes, following the rules of ARF. Hence, s successive successful packet transmissions lead to a transition into state $(i+1)_0$, for $i < N$. On the other hand, f consecutive packet transmission failures lead to a transition into one of two possible states. If, on entering state i_γ , f consecutive packet transmissions fail without any interim successful packet transmissions, then state i_γ is exited with a back-off counter equalling $(\gamma + f) \pmod{\gamma_{max} + 1}$. This back-off counter is carried over to the next state implying a transition to state $(i-1)_{(\gamma+f) \pmod{\gamma_{max} + 1}}$, for $i > 1$. Otherwise, if a successful packet transmission occurs prior to f consecutive failures, the value of the back-off counter at the exit time is $f \pmod{\gamma_{max} + 1}$, implying a transition to state $(i-1)_{f \pmod{\gamma_{max} + 1}}$, for $i > 1$.

When entering state i_γ , the time spent by the process in that state and the transition probabilities to other states are independent of history. Hence, the process is semi-Markovian. Figure 4 shows a state diagram of this process for the case $f = 2$, $N = 3$, and $\gamma_{max} = 5$.

Let μ_{i_γ} represent the expected time (inclusive of overhead) spent in state i_γ and let π_{i_γ} represent the steady-state probabilities of the embedded Markov chain associated with the semi-Markov process. In [22], we detail how to compute these quantities. The analysis is similar to that carried out in the previous sections. In particular, for the case $\gamma = 0$, the transition probabilities out of state i_0 are the same as those out of state i , as given by Proposition 2, and the expected time spent in state i_0 is

$$\begin{aligned} \mu_{i_0} &= \sum_{j=1}^{f-1} \bar{Y}_i(-j) \left(\frac{\bar{\ell}}{R_i} + \bar{T}_b(j \pmod{\gamma_{max} + 1}) \right) + \alpha_i T_{success} + (1 - \alpha_i) T_{failure} \\ &+ \sum_{j=0}^{s-1} \bar{Y}_i(j) \left(\frac{\bar{\ell}}{R_i} + \bar{T}_b(0) \right) + \alpha_i T_{success} + (1 - \alpha_i) T_{failure}, \end{aligned} \quad (29)$$

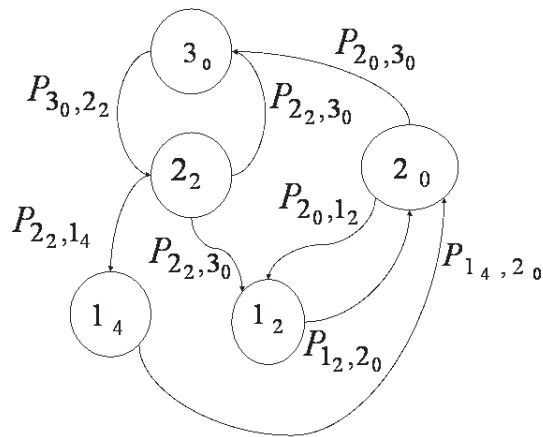


Fig. 4. Embedded Markov chain modeling the behavior of ARF in IEEE 802.11 at the moments of transitions to a new state formulated for specific values of $N = 3$, $f = 2$ and $\gamma_{max} = 5$.

where $\bar{Y}_i(j)$ represents the expected number of visits to state S_j^i , which is defined the same way as in Fig. 2 (i.e., S_j^i corresponds to the state of j consecutive successes or failures, depending on the sign of j , at bit rate R_i). Eq. (29) accounts for both the average transmission time and overhead associated with each visit.

The average throughput of ARF, inclusive of MAC overhead, can now readily be computed. One should note, however, that in each state i_γ the average time spent in actual transmissions, denoted θ_{i_γ} , is shorter than μ_{i_γ} , the total average time spent in that state. The value of θ_{i_γ} is independent of γ and identical to the average time spent in state i by the semi-Markov process of ARF, exclusive of MAC overhead, that was analyzed in Section IV-A (see Proposition 1 and Eq. (5)). Hence, the long-run proportion of time spent by ARF transmitting at rate R_i is given by

$$g_i = \frac{\sum_{\gamma=0}^{\gamma_{max}} \pi_{i_\gamma} \theta_{i_\gamma}}{\sum_{i=1}^N \sum_{\gamma=0}^{\gamma_{max}} \pi_{i_\gamma} \mu_{i_\gamma}}, \quad (30)$$

and the final expression for the average throughput is $\tau = \sum_{i=1}^N g_i \alpha_i R_i$.

V. NUMERICAL RESULTS

In this section, we illustrate the utility of our analysis by numerically comparing the throughput performance of ARF and AARF in two different channel regimes. These results show that neither of these algorithms consistently outperforms the other. We then propose a new variant, called Persistent

AARF (PARFF), that is shown to achieve a good compromise between the two algorithms. Finally, we evaluate the impact of MAC overhead on the respective performance of the algorithms.

A. Performance Comparison of ARF and AARF

We consider a wireless LAN supporting $N = 2$ bit rates, with $R_1 = 1$ Mbps and $R_2 = 2$ Mbps. The parameters of the algorithms are set as follows: $s = 10$, $f = 2$, and, for AARF, $\beta_{max} = 3$. We compare the throughput performance of ARF and AARF under two channel regimes of practical interest. In the first regime, the probability of a successful packet transmission at bit rate R_1 is much higher than at bit rate R_2 , i.e., we fix $\alpha_2 = 0.2$ and evaluate the throughput of ARF and AARF for values of α_1 ranging from 0.7 to 1. In the second regime, the probability of a successful packet transmission at bit rate R_1 is only slightly higher than at bit rate R_2 , that is, we fix $\alpha_2 = 0.7$ and vary α_1 from 0.7 to 1 (note that α_1 should always exceed α_2).

Figure 5 depicts results for the first regime. We observe that AARF outperforms ARF and that the difference between the performance increases with α_1 . The cause of the discrepancy is that ARF attempts too often to switch to the failure prone R_2 bit rate, which results in throughput degradation. On the other hand, AARF spends a lot more time in the optimal R_1 bit rate. This result is consistent with experimental and simulation results reported in [10], [6].

Figure 6 shows results for the second regime and illustrates conditions under which ARF outperforms AARF. The throughput performance of AARF suffers in this region as it tends to spend too much time in the under performing R_1 bit rate, whereas ARF tries to switch to the optimal R_2 much more frequently. This is an insightful result as it indicates the need to optimize AARF under channel regimes where the probability of successful packet transmission is high at both the lower and higher bit rates.

B. Persistent AARF

The main cause of the relatively poor performance of AARF in the second regime is that it is not persistent enough in probing the higher-bit rates. Thus, we propose a simple variation of AARF, called Persistent AARF. PAARF is identical to AARF, except that, when entering a probe state i_{β}^{+1} , it transmits two probe packets at the next higher bit rate instead of just one. If anyone of these two probe packets is successfully transmitted, then PAARF switches to the next higher bit rate, i.e., to state $(i + 1)_0$.

One of the main advantages of our analytical approach is to allow evaluating the performance of such new variants without having to run lengthy simulations. In particular, the analysis of PAARF turns out to

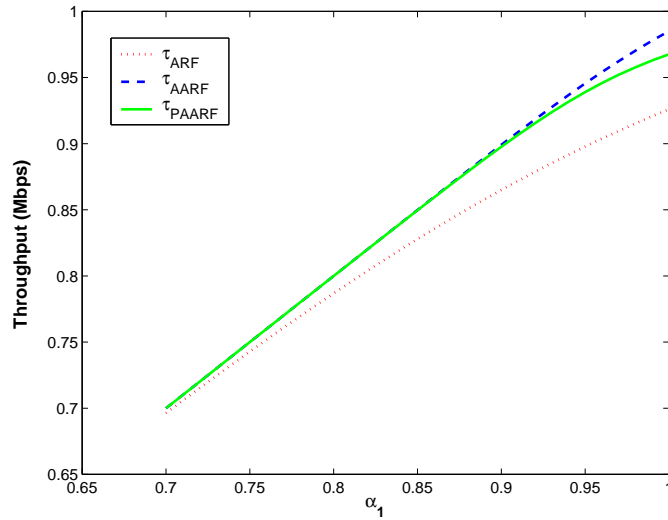


Fig. 5. $R_1 = 1$ Mbps, $R_2 = 2$ Mbps, $\alpha_2 = 0.2$

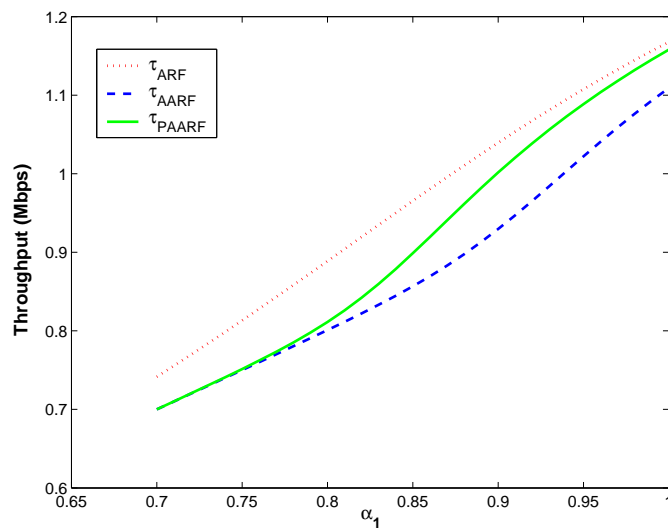


Fig. 6. $R_1 = 1$ Mbps, $R_2 = 2$ Mbps, $\alpha_2 = 0.7$

be almost the same as that of AARF. The only difference is the mean time spent in probe states which is now

$$\mu_{i_\beta}^{i+1} = \frac{(2 - \alpha_{i+1})\bar{\ell}}{R_{i+1}}, \quad (31)$$

and the transition probabilities out of the probe states which become

$$p_{(i_\beta^{i+1}, (i+1)_0)} = 2\alpha_{i+1} - (\alpha_{i+1})^2; \quad p_{(i_\beta^{i+1}, i_{\beta+1})} = 1 - 2\alpha_{i+1} + (\alpha_{i+1})^2, \quad (32)$$

and for the case $\beta = \beta_{max}$,

$$p_{(\beta_{max},(i+1)_0)}^{(i+1)} = 2\alpha_{i+1} - (\alpha_{i+1})^2; \quad p_{(\beta_{max},i_{\beta_{max}})}^{(i+1)} = 1 - 2\alpha_{i+1} + (\alpha_{i+1})^2. \quad (33)$$

Figures 5 and 6 show the performance of PAARF for the two channel regimes in consideration. As one can see, PAARF generally performs close to the best algorithm in each case. One exception is when α_1 is very close to α_2 , in the second regime. In that case, PAARF performs only marginally better than AARF. However, we conjecture that the likelihood of this scenario is relatively low because if the packet success probability at rate R_2 is quite high (e.g., 0.7), then the packet success probability at rate R_1 is likely to be close to 1.

C. Impact of MAC Overhead and Transmission Rates

We next evaluate the effects of MAC overhead on the performance of the various algorithms. We present numerical results based on the analysis of Section IV-C. The protocol parameters are set according to the specifications of the IEEE 802.11 standard, that is, $\gamma_{max} = 5$, $DIFS = 50 \mu s$, $SIFS = 10 \mu s$, $T_{ACK} = 112 \mu s$, and $CW_{min} = 32$ [2]. The other algorithm, operational and channel parameters remain the same as in the previous sections.

Figures 7 and 8 show the performance of ARF, AARF and PAARF, respectively for $\alpha_2 = 0.2$ and $\alpha_2 = 0.7$. The bit rates are set to $R_1 = 1$ Mbps and $R_2 = 2$ Mbps. The results show that MAC overhead reduces the achieved throughput of all the three algorithms. However their underlying behavior remains the same as previously.

We next illustrate the effect of the bit rates on the behavior of the three algorithms. For this, we again analyze their delivered throughput under the previously mentioned channel regimes, but this time with bit rates $R_1 = 5.5$ Mbps and $R_2 = 11$ Mbps.

Figure 9 show the performance of ARF, AARF and PAARF for $\alpha_2 = 0.2$. We can see that the relative performance of ARF with respect to the other algorithms is considerably worse at higher rates. This can be attributed to the fact that MAC overhead time does not scale with the transmission rate. Hence, at high data rate, the impact of MAC overhead due to a failed transmission gets magnified. Consequently, ARF with its higher tendency to switch to the poor performing rate R_2 experiences a relatively larger performance degradation than the other algorithms.

Figure 10 shows the performance of the three algorithms in the second regime, i.e., $\alpha_2 = 0.7$. The

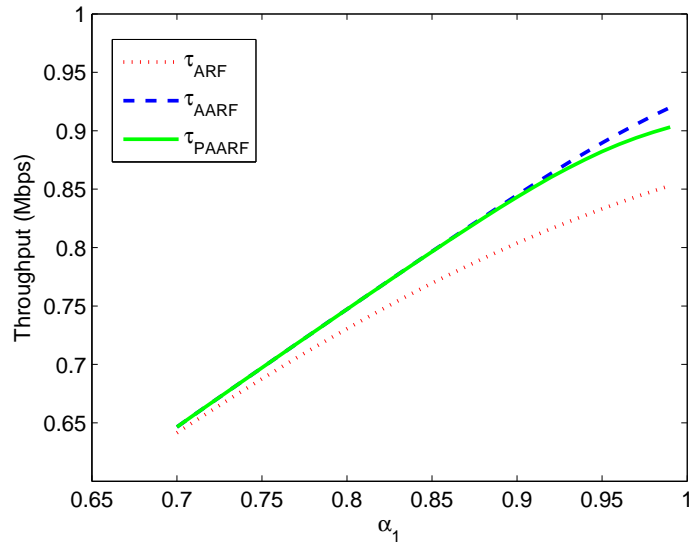


Fig. 7. $R_1 = 1$ Mbps, $R_2 = 2$ Mbps, $\alpha_2 = 0.2$ with MAC overhead

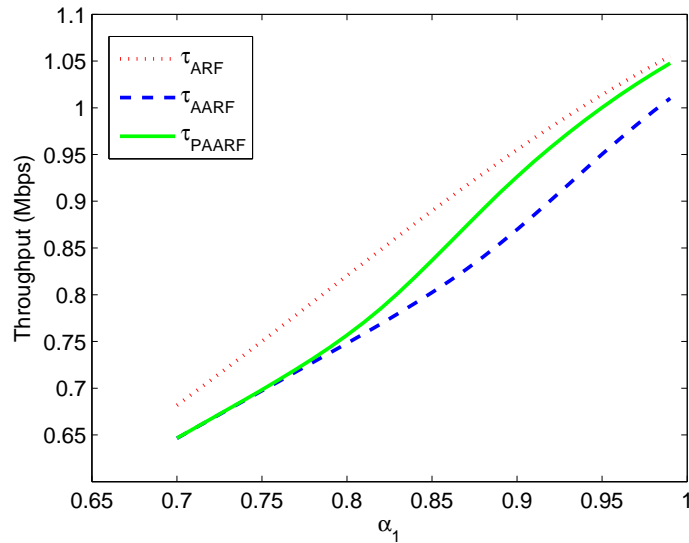


Fig. 8. $R_1 = 1$ Mbps, $R_2 = 2$ Mbps, $\alpha_2 = 0.7$ with MAC overhead

nature of the results in this region is similar to those shown in Fig. 6, though the superiority of ARF is not as pronounced. In fact, as α_1 tends to 1, PAARF starts outperforming ARF. Overall, these results show that PAARF keeps providing a good trade-off between ARF and AARF, even when taking MAC overhead into consideration.

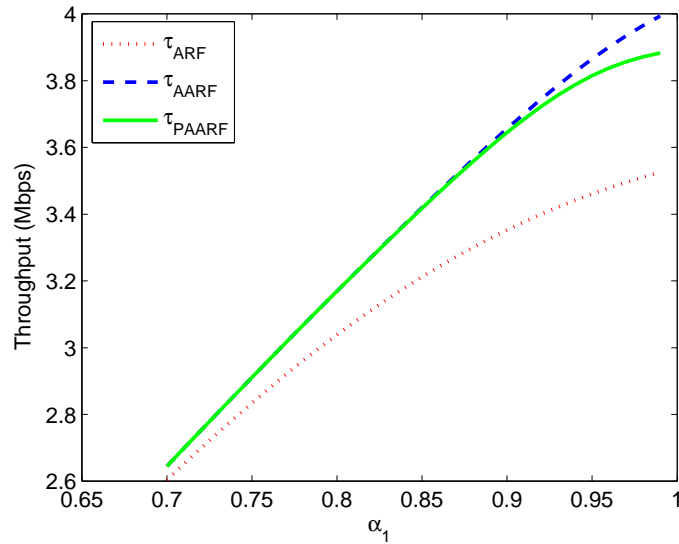


Fig. 9. $R_1 = 5.5$ Mbps, $R_2 = 11$ Mbps, $\alpha_2 = 0.2$ with MAC overhead

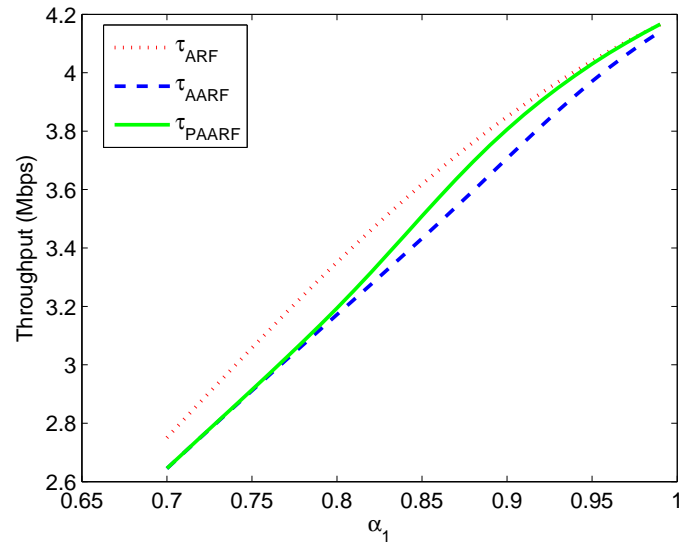


Fig. 10. $R_1 = 5.5$ Mbps, $R_2 = 11$ Mbps, $\alpha_2 = 0.7$ with MAC overhead

VI. CONCLUSIONS

In this paper, we proposed a novel semi-Markovian framework to analyze the performance of two of the most widely implemented rate adaptation algorithms in wireless LANs, namely ARF and AARF. Given our modeling assumptions, the analysis is exact and provides closed form expressions for the achievable throughput of ARF and AARF. A particularly interesting finding was that the multi-dimensional embedded

Markov chain associated with the semi-Markov process of AARF collapses into a simple one dimensional birth-death process.

We used the analytical expressions to numerically compare the throughput performance of ARF and AARF in two channel regimes for a wireless LAN operating at two different bit rates. We found that none of the algorithms consistently prevails over the other. Based on this insight, we devised a new variant to AARF, called Persistent AARF (PAARF), whereby two probe packets (instead of just one) are transmitted each time the algorithm enters one of the probe states. We were able to analyze PAARF much the same way as AARF and our numerical results showed that this simple modification can significantly improve the performance of AARF in the regime where it does not perform well, while maintaining almost the same performance in the regime where it does perform well.

Next we analyzed the impact of the IEEE 802.11b MAC overhead on the performance of ARF, AARF and PAARF by numerically comparing their throughput performance based on the analysis presented in section IV-C. The results revealed that, at low bit rates, MAC overhead does not alter the basic behavior of the three algorithms and contributes only in reducing the achieved throughput. However, MAC overhead becomes increasingly significant as the bit rate increases. This is because the exponentially increasing back-off time accompanying failed packet transmissions becomes particularly significant at high bit rates. This phenomenon translates into a performance edge for AARF and PAARF, as the bit rates increase.

The analytical framework developed in this paper provides the basis for many other interesting types of optimizations. For instance, an important issue is how to optimally set the operational parameters of ARF and AARF. Another important area for future work is to numerically evaluate the performance of ARF, AARF, and PAARF for more than two bit rates. Overall, this work marks a first step in modeling rate adaptation in wireless LANs and shows promise for analytically evaluating other open-loop rate adaptation algorithms, especially those based on ARF.

REFERENCES

- [1] Z. J. Haas, J. Deng, B. Liang, P. Papadimitratos, and S. Sajama, "Wireless ad hoc networks," in *Encyclopedia of Telecommunications*, J. G. Proakis, Ed. Wiley, 2002.
- [2] "ANSI/IEEE Std 802.11-1999 Wireless LAN Medium Access Control (MAC) and Physical Layer (PHY) Specifications," 1999.
- [3] S. Ray, J. B. Carruthers, and D. Starobinski, "Evaluation of the masked node problem in ad-hoc wireless LANs," *IEEE Transactions on Mobile Computing*, vol. 4, no. 5, pp. 430–442, September/October 2005.
- [4] V. Saligrama and D. Starobinski, "On the macroscopic effects of local interactions in multi-hop wireless networks," in *WiOpt '06*, 2006.
- [5] A. Kamerman and L. Monteban, "WaveLAN[R]-II: A high-performance wireless LAN for the unlicensed band," *Bell Labs Technical Journal*, vol. 2, no. 3, pp. 118–133, August 1997.

- [6] M. Lacage, H. M. Manshaei, and T. Turletti, "IEEE 802.11 rate adaptation: A practical approach," in *MSWiM '04*, October 2004, pp. 126–134.
- [7] G. Holland, N. Vaidya, and P. Bahl, "A rate-adaptive MAC protocol for multi-hop wireless networks," in *MobiCom 2001*, July 2001, pp. 236–251.
- [8] S. Wong, S. Lu, H. Yang, and V. Bharghavan, "Robust rate adaptation for 802.11 wireless networks," in *MobiCom 2006*, 2006, pp. 146–157.
- [9] J. Kim, S. Kim, S. Choi, and D. Qiao, "CARA: Collision-aware rate adaptation for IEEE 802.11 WLANs," in *Proceedings of IEEE INFOCOM'2006*, April 2006.
- [10] J. Bicket, "Bit-rate selection in wireless networks," Master's thesis, Massachusetts Institute of Technology, February 2005.
- [11] S. Ross, *Stochastic Processes*, 2nd ed. Wiley, 1996.
- [12] P. Chevillat, J. Jelitto, A. N. Barreto, and H. Truong, "A dynamic link adaptation algorithm for IEEE 802.11a wireless LANs," in *Proceedings of the IEEE ICC*, May 2003, pp. 1141–1145.
- [13] D. Qiao and S. Choi, "Fast-responsive link adaptation for IEEE 802.11 WLANs," in *Proceedings of the IEEE ICC*, May 2005.
- [14] M. H. Manshaei and T. Turletti, "Simulation-based performance analysis of 802.11a wireless LAN," in *Proceeding of International Symposium on Telecommunications*, August 2003.
- [15] D. Qiao, S. Choi, and K. G. Shin, "Goodput analysis and link adaptation for IEEE 802.11a wireless lans," *IEEE Transactions on Mobile Computing*, vol. 1, no. 4, pp. 278–292, October-December 2002.
- [16] Y. Xi, J. Wei, and Z. Zhuang, "Rate adaptive transmission scheme for IEEE 802.11 WLANs," *Journal of Communication and Computer*, vol. 3, no. 1, January 2006.
- [17] D.-Y. Yang, T.-J. Lee, K. Jang, J.-B. Chang, and S. Choi, "Performance enhancement of multirate IEEE 802.11 WLANs with geographically scattered stations," *IEEE Transactions on Mobile Computing*, vol. 5, no. 7, pp. 906–919, July 2006.
- [18] G. R. Cantieni, Q. Ni, C. Barakat, and T. Turletti, "Performance analysis under finite load and improvements for multirate 802.11," *Computer Communications Journal, special issue on Performance Issues of Wireless LANs, PANs, and Ad Hoc Networks*, vol. 28, no. 10, pp. 1095–1109, June 2005.
- [19] J. Choi, K. Park, and C. Kim, "Cross-layer analysis of rate adaptation, DCF and TCP in multi-rate WLANs," in *Proceedings of IEEE INFOCOM 2007*.
- [20] A. Singh and D. Starobinski, "A semi Markov-based analysis of rate adaptation algorithms in wireless lans," in *Proceedings of IEEE SECON 2007*, June 2007.
- [21] A. Balachandran, M. G. Voelker, P. Bahl, and P. V. Rangan, "Characterizing user behavior and network performance in a public wireless LAN," in *SIGMETRICS 2002*, June 2002, pp. 195–205.
- [22] A. Singh, "An exact analysis of rate adaptation in wireless local area networks," Master's thesis, Boston University, July 2007.